Chem Biol Drug Des 2012; **79:** 431–441

Research Article

doi: 10.1111/j.1747-0285.2011.01281.x

A Novel Pharmacophore Model to Identify Leads for Simultaneous Inhibition of Anti-coagulation and Anti-inflammatory Activities of Snake Venom Phospholipase A_2

Abdul Wadood[1,3], Syed Abid Ali[2], Rabia Sattar[1], Muhammad Arif Lodhi[2] and Zaheer Ul-Haq[1,*]

[1]Dr Panjwani Center for Molecular Medicine and Drug Research, International Center for Chemical and Biological Sciences, University of Karachi, Karachi 75270, Pakistan

[2]HEJ Research Institute of Chemistry, International Center for Chemical and Biological Sciences, University of Karachi, Karachi 75270, Pakistan

[3]Department of Biochemistry, Shankar Campus, Abdul Wali Khan University, Mardan, Pakistan

**Corresponding author: Zaheer Ul-Haq, zaheer.qasmi@iccs.edu*

In addition to catalytic action, snake venom phospholipase A_2 induces several pharmacological effects including neurotoxicity, cardiotoxicity as well as anti-coagulant and anti-platelet aggregation effects. Therefore, strategy to identify dual inhibitor for this enzyme will be of much importance in medical research. In this paper, structure-based pharmacophore mapping, molecular docking, protein–ligand interaction fingerprints, binding energy calculations, and binding affinity predictions were employed in a virtual screening strategy to identify new hits for dual inhibition of anti-coagulation and inflammation of phospholipase A_2. A structure-based pharmacophore map was modeled which comprised of important interactions as observed in co-crystal of phospholipase A_2 and its dual inhibitor indomethacin. The generated model was used to retrieve molecules from ChemBridge, a free database of commercially available compounds. A total of 381 molecules mapped on the developed pharmacophore model from ChemBridge database. The hits retrieved were further screened by molecular docking, protein–ligand interaction fingerprints, binding energy calculations, and binding affinity predictions using Genetic Optimization for Ligand Docking and MOE. Based on these results, 32 chemo-types molecules were predicted as potential lead scaffolds for developing novel, potent and structurally diverse dual inhibitor of phospholipase A_2.

Key words: docking, dual inhibitor, pharmacophore, phospholipase A_2, snake, venom, virtual screening

Received 14 March 2011, revised 30 September 2011 and accepted for publication 25 November 2011

Phospholipase A_2 (PLA_2) is an important family of different enzymes that exhibits diverse substrate specificities, subcellular localization, requirements of cofactor, and cellular function (1). The PLA_2 class of enzymes especially catalyzes the hydrolysis of the 2-acyl ester bond of phospholipids to yield arachidonic acid that is used as a substrate by cyclooxygenase (COX) and lipoxygenase enzymes, as a result eicosanoids is formed (2,3). Snake venom PLA_2, in addition to catalytic action, also mediates several pharmacological disorders, for example, myotoxicity, neurotoxicity, cardiotoxicity as well as anti-coagulant, edema inducing, hemolytic and platelets modulating effects (4). The primary consideration is that the catalytic properties and pharmacological actions were related, and all the activities were based on the specific and critical phospholipids hydrolysis (5). Alternatively, it has been reported that the pharmacological properties of snake venom PLA_2 are not necessarily dependent on their catalytic activity, and it might be due to the protein–protein interactions involving a specific site on the surface of protein (6,7). So far, these pharmacological sites are neither clearly defined nor their binding modes are established. Consequently, the effective chemical entities have not been designed to prevent the interactions of these sites to overcome the harmful pharmacological effects, whereas the substrate binding region and the residues involved in the catalytic activities of PLA_2 enzymes are well established. A number of three-dimensional (3D) structures of different PLA_2 isoforms from a variety of sources have been recently resolved (8–18). To understand the mechanism of catalytic actions of PLA_2, a number of inhibitors have been designed for the inhibition of their enzymatic activity. Several complex structures of PLA_2 with natural compounds, synthetically designed inhibitors as well as substrate analogues, have also been published (9,19–26). It has also been reported that the anti-inflammatory activity showed by non-steroidal anti-inflammatory drugs has been attributed to their binding to PLA_2 and COX enzymes (27–33).

The anti-coagulant activity in snake venom PLA_2 was also reported many years ago by Buffa *et al.* (34,35). It has been reported that the anti-coagulant activity in various snake venom PLA_2 is greatly varied. Based on their activities, the PLA_2 was further classified into strong, weak, and non-coagulant compounds (4,36). It has also been suggested that the anti-coagulant site exists between residues 54–77. Although the exact nature of the structure of this

anti-coagulant loop is not clearly understood so far, it has been shown that the strong anti-coagulant activity of PLA_2 attributed to the presence of basic residues at precise positions in the segment 54–77. For example, isoform of PLA_2 from *Daboia russelli pulchella* possesses five basic residues in the loop 54–77 demonstrating its potential to be powerful anti-coagulant. However, the ligand-binding mode for inhibiting the anti-coagulant activity of PLA_2 is not fully understood, and hence, the ligand could not be designed to inhibit the anti-coagulant action of PLA_2. Indomethacin has been reported long time ago as a non-selective COX-2 inhibitor (37). In recent studies, it has also been reported that indomethacin inhibits group II PLA_2, but its unusual kinetic properties could not be explained (38,39). These studies demonstrate that the binding mode of indomethacin is very different as compare to other molecules that bind to the substrate binding site of PLA_2 enzyme. It was also indicated that indomethacin blocks the anti-thrombotic action of PLA_2, thus suggesting that indomethacin might also be involved in inhibiting its anti-coagulant binding site (40). Very recently, the co-crystallized structure of PLA_2 with indomethacin has been resolved, to understand its binding mode with PLA_2 and the mechanisms of its actions against both catalytic and anti-coagulant actions. A remarkable new ligand-binding site has been identified, which demonstrates that indomethacin binds to the amino acid residues that are significant for the catalytic action of the enzyme as well as for its anti-coagulant activity.

In recent years, high-throughput virtual screening has been emerging as a complementary to high-throughput screening in an attempt to discover novel potential lead compounds in the process of drug discovery (41). Thus, to identify new and potent compounds that inhibit both the catalytic and anti-coagulant activities of snake venom PLA_2 like indomethacin, structure-based pharmacophore modeling and virtual screening may consider as an effective approach. This paper describes the structure-based pharmacophore modeling to identify the pharmacophoric features required for simultaneous inhibition of anti-coagulant and inflammatory effects by virtual screening, molecular docking, protein–ligand interaction fingerprints (PLIFs), binding energy calculations, and binding affinity predictions.

Materials and Methods

Generation of structure-based pharmacophore model

In the present study, the only crystal structure of PLA_2 in complex with a dual inhibitor indomethacin (3H1X.pdb) was used as starting structure for the generation of structure-based pharmacophore models (42). LigandScout (LS) is a tool that allows the automatic construction and visualization of 3D pharmacophore from structural data of macromolecules/ligand complexes (43). For the LS algorithm, chemical features include hydrogen bond donors and acceptors as directed vectors, and positive and negative ionizable regions as well as lipophilic areas are represented by spheres. Moreover, to increase the selectivity, the LS model includes spatial information regarding areas inaccessible to any potential ligand, thus reflecting possible steric restrictions. In particular, excluded volume spheres placed in positions that are sterically forbidden are automatically added to the generated pharmacophore model. The software LS was applied to the detection and interpretation of crucial interaction patterns between PLA_2 and ligand. LS extracts and interprets ligands and their macromolecular environment from PDB files and automatically generates and visualizes advanced 3D pharmacophore models.

LigandScout may also be used to construct pharmacophore of varying degrees of sophistication, suitable for export to different programs. In the present study, MOE-compatible 3D-pharmacophore model was first developed by LS using default parameters, and then, it was exported and converted into a Molecular Operating Environment, pharmacophore query for virtual screening (http://www.chemcomp.com). Prior to screening, it was necessary to make a number of adjustments, because feature interpretation differs slightly between the two programs. Those aromatic rings that LS classified simply as hydrophobic groups were classified as either aromatic or hydrophobic in MOE, using the PPCH_All scheme (which incorporates directionality of hydrogen bond donors and acceptors, and orientation of aromatic rings). As in LS pharmacophore, the aromatic ring is not directly classified as such (because of lack of detection of π–π stacking or cation–π interactions) but rather as a set of hydrophobic atoms, can be interpreted in MOE in a manner that is useful in the prediction of right compounds in virtual screening.

Pharmacophore-based virtual screening

The ChemBridge database (http://www.chembridge.com), which allows the user to download compounds structures from a variety of vendors as SDF files, was used in this preliminary screen. Using MOE, the database was washed, and the 3D structure of each compound was built using the MMFF94x force field. Then for each compound, the low-energy conformers were generated using Conformation Import methodology implemented in MOE software. After assessing the pharmacophore query, virtual screening was carried out using the software MOE against ChemBridge database. Because some changes may occur when the pharmacophore is exported from LS to MOE environment, therefore, the pharmacophore queries were validated before using it for virtual screening. To reduce the data of identified hits, they were docked into the recently identified binding pocket of PLA_2, and the PLIFs were developed using MOE. Binding energies and binding affinities were calculated using LigX (Chemical Computing Group, Montreal, Quebec, Canada) implemented in MOE to prioritize the final hits.

Molecular docking

Molecular docking studies were performed using Genetic Optimization for Ligand Docking (GOLD) from Cambridge Crystallographic Data Center, UK (44). GOLD uses genetic algorithm for docking flexible small molecules (ligands) into binding site of macromolecules (target proteins) to investigate the full range conformational flexibility of ligand with partial flexibility of the receptor. The ligand-binding energy with receptor was predicted via GOLD score implemented in GOLD. The total GOLD score, which is represented as 'Fitness', was calculated from the contribution of hydrogen bonds and van der Waals interactions between receptor and ligand as well as the contribution of intra-molecular hydrogen bonds and intra-molecular strain in the

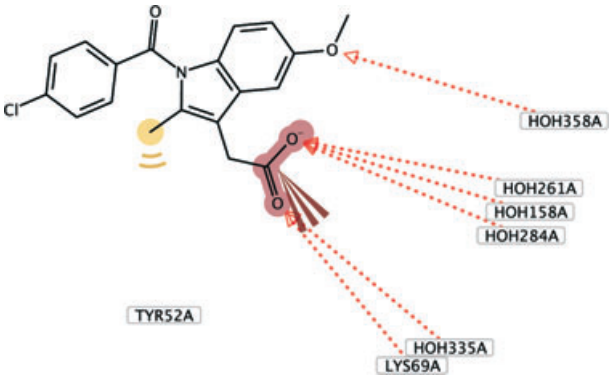

Figure 1: Two-dimensional pharmacophore model generated by LIGANDSCOUT from the complex structure of phospholipase A_2 and indomethacin. The dotted arrows indicated the hydrogen bond acceptor features, and the yellow sphere represented the hydrophobic feature in the ligand.

ligand. Receptor co-ordinates of the crystal structure of PLA_2-inhibitor complex were used to define the binding site for molecular docking studies. All the solvent molecules except involved in ligand binding (i.e. W158, W261, and W284) in the crystal structure were removed, and hydrogen atoms were added to the whole protein. The ligand-binding site for docking was defined as a collection of amino acids enclosed within a sphere of 10 Å radius around the co-ordinates of indomethacin, which is the inhibitor molecule present in the binding site of PLA_2-inhibitor complex. Top 10 docked poses were allowed to be saved with the early termination option of quitting the genetic optimization calculation for a ligand if the RMSD between any five conformations of the particular ligand is <1.5 Å. All other parameters were kept at their default values. Molecular interactions were observed using PLIF and LIGX software implemented in MOE.

Computation of generalized Born interaction energies and binding affinity

To predict the most promising compounds, binding affinities of the hits-PLA_2 complexes were calculated with generalized Born/volume integral (GB/VI) implicit solvent method using LIGX tool in MOE (45).[a] Generalized Born interaction energy is the non-bonded interaction energy between the macromolecule and the ligand, which comprises van der Waals, Coulomb electrostatic interaction, and implicit solvent interaction energies; however, ligand and receptor macromolecule strain energies are not taken into account. LIGX is the name for a collection of procedures and capabilities in MOE for conducting interactive ligand modification and energy minimization in the binding pocket of a flexible receptor. In LIGX calculations, the receptor atoms far from the ligand are held fixed (constrained not to move) while receptor atoms in the vicinity of the ligand (in the active site) are allowed to move but are subject to tether restraints that discourage gross movement. The ligand atoms can be configured as either free to be move or subject to similar tethers as the receptor. Prior to calculation of binding energy, binding pocket of PLA2 and the ligand in the complex were subjected to energy minimization. During the minimization, the positions of residues of PLA2 that are located 10 Å away from ligand were constrained. The calculated binding affinities of each compound are reported in the units of pki.

Results and Discussion

Generation of structure-based pharmacophore model

As shown in Figures 1 and 2B, the pharmacophore model automatically generated by the LS program includes four features: three hydrogen bond acceptors (HBA) and one hydrophobic group. Besides, the program automatically generated several excluded volumes in the model. The HBA features points toward the carboxylic and methoxy oxygen atoms of the ligand from the Lys^{69} and water molecules W158, 261, 284, and 358, respectively. The hydrophobic groups are located on the methyl group adjacent to the indole ring of the ligand. The developed pharmacophore model was exported into MOE. Prior to screening, it was necessary to make a number of adjustments, as feature interpretation varies slightly between the two programs. As in LS pharmacophore, the aromatic ring of the compound in the complex was not classified as aromatic or hydrophobic features; thus, these were interpreted in MOE, using the PPCH_All scheme. Two modifications were made on this model to obtain appropriate model for virtual screening. The first modification is about the chlorobenzyl ring. It is clear that it is an aromatic group, but the LS could not interpret this ring as an aromatic group automatically. In MOE, additional features were developed using the MOE pharmacophore query editor. First, an aromatic feature was developed on the chlorobenzyl ring, and a hydrophobic feature was developed on the phenyl ring of indole moiety of the ligand. This modified pharmacophore model was then validated by screening the test database. In the test database, we kept the compound (i.e. indomethacin) present in complex structure. First, the indomethacin was extracted, and then, hydrogen atoms were added and energy minimized by using MOE. The minimized structure of indomethacin was added to the test database. After screening, the test compound was correctly mapped by the modified pharmacophore model as shown in Figure 2A. The result verified the validity of our modified pharmacophore model that can be used for the screening of large databases.

Pharmacophore-based virtual screening

The modified validated pharmacophore model was then used as *in silico* filter to screen the ChemBridge database (http://www.chembridge.com) of commercially available compounds. The ChemBridge database compounds in SDF format were loaded into MOE environment where the 3D structure of each compound was modeled using MMFF94x force field. The Conformation Import methodology was applied to generate low-energy conformations for each compound. All these compounds and their respective conformations were saved in MOE database. The conformers of each compound were then filtered by the pharmacophore model. To be considered as hit, the compound has to fit all the features of the pharmacophore. From the pharmacophore-based virtual screening, 381 hits were identified that mapped on the developed pharmacophore model (i.e. having the specified requirements). These initially identified hits were selected for further evaluation using docking studies.

Table 1: GOLD fitness scores, binding energies, and binding affinities of most promising lead compounds. See Materials and Methods for details

S. no.	Compound structure	GOLD score	Binding energy (MM/GBVI kcal/mol)	Binging affinity (pki)
1	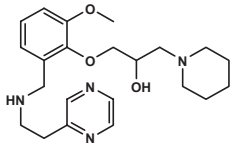	53.79	−16.98	8.41
2	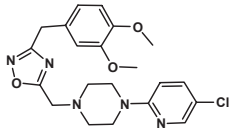	63.24	−18.27	7.43
3	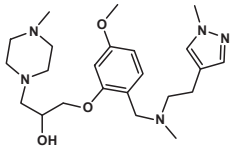	53.69	−17.35	7.84
4	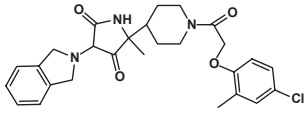	47.37	−13.82	8.25
5	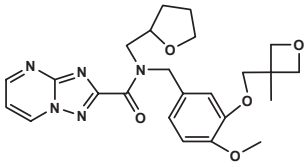	57.97	−16.77	7.12
6	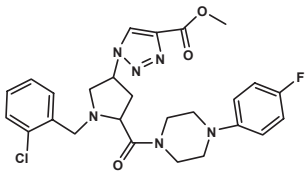	48.62	−14.65	5.66
7	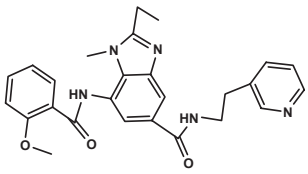	48.24	−21.31	7.23
8	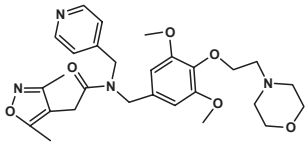	59.56	−19.68	7.35
9	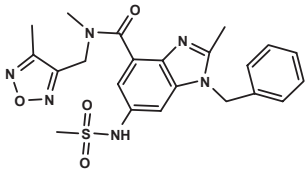	55.24	−17.47	6.62

Table 1: (*Continued*)

S. no.	Compound structure	GOLD score	Binding energy (MM/GBVI kcal/mol)	Binging affinity (pki)
10	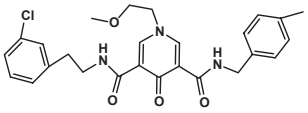	59.82	−19.46	7.40
11	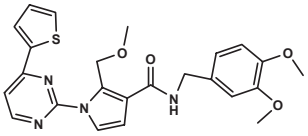	66.57	−17.69	9.47
12	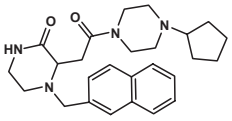	47.54	−14.35	8.22
13	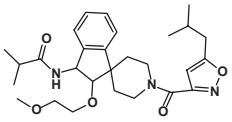	46.77	−16.45	6.49
14	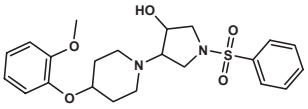	67.76	−22.50	9.12
15	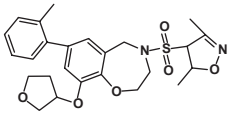	50.60	−21.31	7.60
16	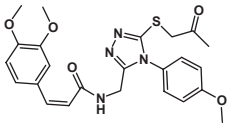	63.90	−23.21	6.76
17	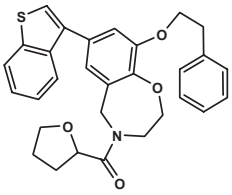	58.16	−21.38	7.71
18	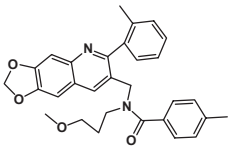	48.16	−21.10	7.07
19	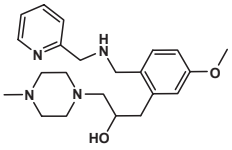	52.53	−24.66	8.46

Table 1: (*Continued*)

S. no.	Compound structure	GOLD score	Binding energy (MM/GBVI kcal/mol)	Binging affinity (pki)
20	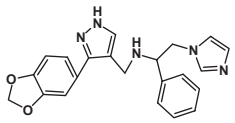	59.18	−17.48	8.18
21	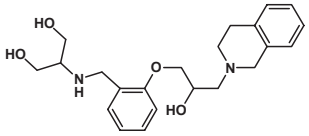	55.22	−16.20	8.16
22	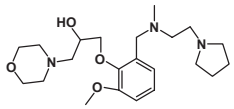	47.22	−13.90	6.58
23	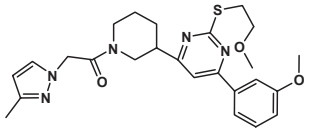	60.46	−20.41	8.49
24	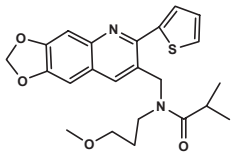	49.78	−13.88	7.23
25	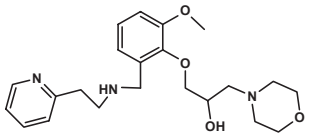	52.78	−15.53	7.93
26	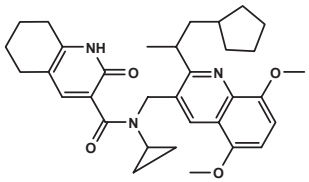	51.20	−18.91	6.39
27	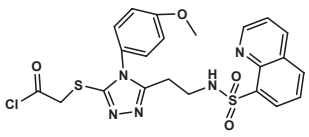	65.73	−17.79	9.15
28	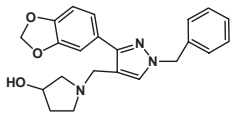	53.54	−17.78	8.30
29	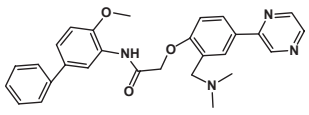	58.25	−20.39	8.59

Table 1: (*Continued*)

S. no.	Compound structure	GOLD score	Binding energy (MM/GBVI kcal/mol)	Binging affinity (pki)
30	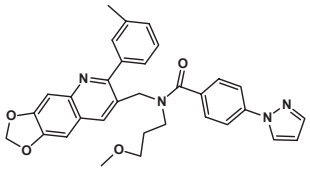	52.22	−20.51	7.37
31	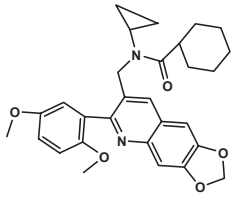	55.99	−13.38	7.25
32	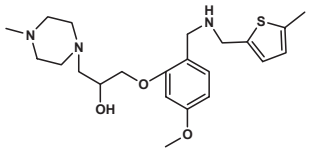	57.92	−25.17	7.15
Indomethacine	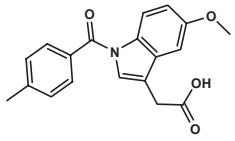	58.00	−13.28	6.98

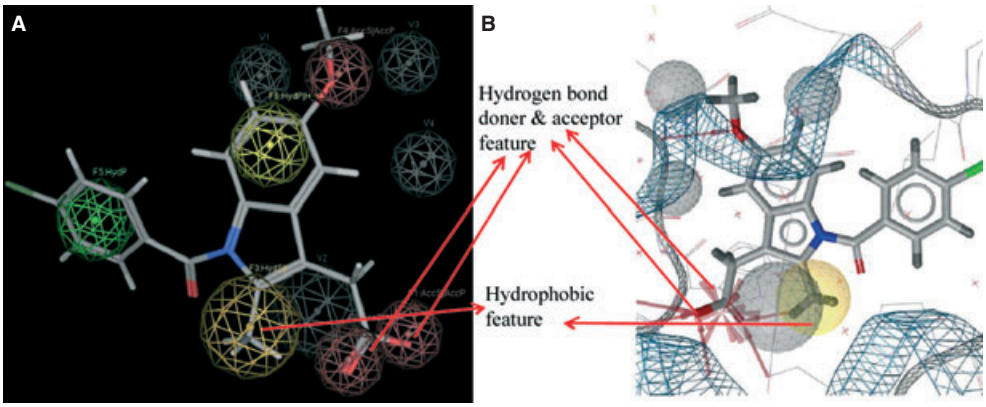

Figure 2: (A) Three-dimensional pharmacophore model generated by LIGANDSCOUT from the complex structure of phospholipase A_2 and indomethacin. The red arrows indicate the hydrogen bond acceptor features, the yellow sphere indicates the hydrophobic feature in the ligand, whereas the gray spheres represent the restricted volume in the receptor. (B) The fitting of indomethacin on modified three-dimensional pharmacophore model developed by using MOE pharmacophore query editor. The pink, green, and yellow color spheres indicated hydrogen bond acceptor, aromatic and hydrophobic features, respectively, whereas the gray color spheres represented the excluded volumes.

Molecular docking

To deduce the promising compounds for dual inhibitors of PLA_2, all the initial hits were docked into the recently identified binding pocket of PLA_2 using the automated GOLD docking program. Prior to dock the initial hits, the ligand (i.e. indomethacin) from the complex structure was extracted and re-docked into the binding pocket to validate the docking protocol. The docked conformation corresponding to the high GOLD fitness score was selected as the most promising binding conformation. The root mean square deviation (RMSD) between the docked and experimentally determined conformation was calculated

using SVL script of MOE and found to be equal to 1.33 Å, suggesting that a high docking reliability of GOLD in reproducing the experimentally determined binding mode for PLA_2. The GOLD docking software and the parameters set could be extended to search the PLA_2 binding conformations for other compounds accordingly. Using the same docking protocol, all the initial hits were docked into the binding pocket of PLA_2. Furthermore, on the basis of GOLD fitness score, the top-ranked 100 compounds were selected for further detail investigations. For the top-ranked pose of all the selected compounds, PLIFs were generated by MOE, and those compounds that revealed significant interactions with important residues of recently identified binding pocket (i.e. Asp^{49}, His^{48}, Lys^{69}) and water molecules in the catalytic and anti-coagulant active site regions of PLA_2 were picked as promising hits. Protein–ligand interaction fingerprints implemented on MOE classify the interactions between a ligand and the residues on the binding site into various types of weak and strong interactions. Among the top-ranked 100 compounds, 53 compounds showed the crucial interaction with the enzyme via PLIFs.

Computation of binding affinity and expert visual inspection

Finally, binding energy and binding affinity for all the 53 compounds including indomethacin were calculated using LIGX implemented in MOE to prioritize identified promising hits. The criteria for the selection of the most promising hits were compounds having binding energy and binding affinity equal to or good as compare to the binding energy and binding affinity calculated for indomethacin, visualization of each compound in the binding pocket and the selection of only those compounds exhibiting interactions with both catalytic and anti-coagulation region of PLA_2, and diversity of the compounds. Applying the above-mentioned criteria, 32 compounds of 53 fulfill the specific requirements summarized in Table 1. The pharmacophore mapping, PLIFs, binding mode, binding energy, and binding affinity prediction showed that these predicted lead hits might act as good lead compounds for the development of novel, potent, and structurally diverse dual inhibitors of snake venom PLA_2 enzyme.

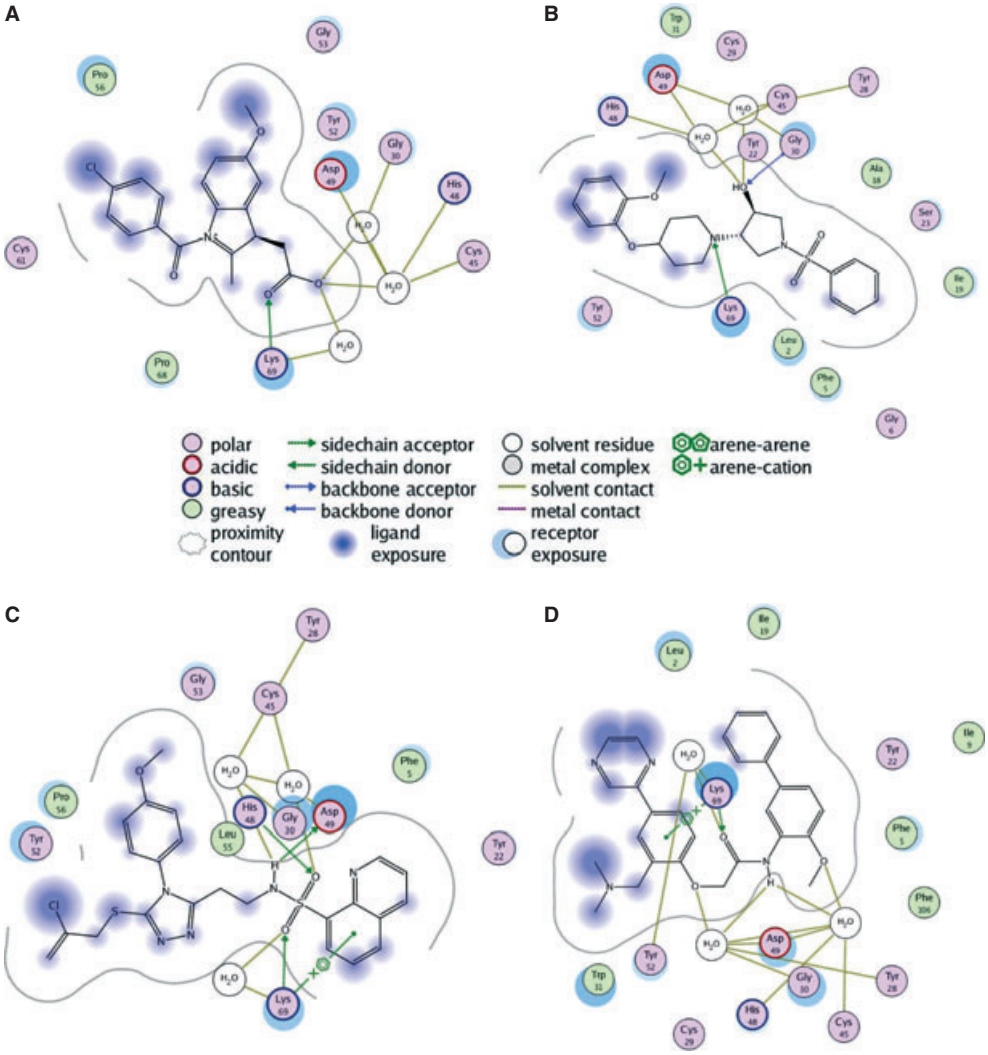

Figure 3: Two-dimensional representations of the interactions of (A) indomethacin, (B) compounds **14**, (C) compound **27**, and (D) compound **29** and snake venom phospholipase A_2. Hydrogen bonds are represented with green dashed lines.

Binding interactions of finally selected compounds

The docking studies revealed that almost all finally selected lead hits showed similar binding interactions as that of indomethacin to both catalytic and anti-coagulant regions of PLA_2 enzyme. For example, compound **14** for which the strong binding affinity (09.1 pki), lower binding energy (−22.5), and high GOLD fitness score (67.76) were observed showed the binding interaction similar to that of indomethacin (Table 1). From the docked conformation, it was also predicted that the oxygen atom of hydroxyl group attached to the pyrrolidine ring and nitrogen atom in pyridine ring of the compound **14** established interaction with the amino acid residues Asp^{49}, Gly^{30}, His^{40}, and Lys^{69} in a similar manner of indomethacin to the same residues (Figure 3A,B). Similarly, it was also predicted that the oxygen atoms attached to the sulfur atom in compound **27** interact in the same fashion to the important residues of the enzyme (Figure 3C). Likewise, in the binding mode of compound **29**, oxygen atom of methoxy group attached to the phenyl ring of the compound interacts with the catalytic region, whereas the carbonyl oxygen interacts with anti-coagulant region of PLA_2 in a similar fashion as indomethacin (Figure 3D). From the docking poses of the selected compounds, it was observed that there are some specific functional groups that interact with the catalytic and anti-coagulation regions and fit well in the newly identified binding pocket of snake venom PLA_2 enzyme.

Conclusion

The aim of this study was to generate a pharmacophore model to identify structurally diverse lead hits. The identified hits might be used for developing novel and potent inhibitors for simultaneous inhibition of anti-coagulant and inflammatory affects of snake venom enzyme PLA_2. A structure-based pharmacophore was developed based on the complex structure of PLA_2 and indomethacin. The developed pharmacophore model was used for the screening of ChemBridge database. The identified hits were further evaluated by molecular docking, PLIFs development, binding energy calculation, and binding affinity prediction. As a result, 32 lead hits were reported that fulfilled all the criteria for the design of compounds that might act as good leads for development of novel, potent, and structurally diverse compounds for dual inhibition. From the binding mode, predicted by docking, it was observed that there are some specific groups that mimic the binding mode of indomethacin and fit well to both of the catalytic and ant-coagulation region of PLA_2 enzyme. Further studies toward the synthesis and structure–activity relationship of the above-mentioned lead compounds with different snake venom PLA_2 are in progress and will be reported elsewhere.

Acknowledgments

Financial support from ASEA-UNINET under the Austrian-Pakistan Cooperation Project in Computational Chemistry (APCPC) is highly acknowledged. We are extremely grateful to Dr Reaz uddin (Dr Panjwani Center for Molecular Medicine and Drug Research, University of Karachi, Pakistan) for his useful suggestions and meaningful discussions.

References

1. Dennis E.A. (1997) The growing phospholipase A_2 superfamily of signal transduction enzymes. Trends Biochem Sci;22:1–2.
2. Smith W.L., De Witt D.L., Garavito R.M. (2000) Cyclooxygenase: structural, cellular, and molecular biology. Annu Rev Biochem;69:145–182.
3. Dennis E.A. (1983) Phospholipases. In: Boyer P., editor. The Enzymes. New York: Academic Press; p. 307–353.
4. Kini R.M., Evans H.J. (1987) Structure-function relationships of phospholipases. The anticoagulant region of phospholipases A_2. J Biol Chem;262:14402–14407.
5. Rudrammaji L.M., Machiah K.D., Kantha T.P., Gowda T.V. (2001) Role of catalytic function in the antiplatelet activity of phospholipase A_2 cobra (*Naja naja naja*) venom. Mol Cell Biochem;219:39–44.
6. Kerns R.T., Kini R.M., Stefansson S., Evans H.J. (1999) Targeting of venom phospholipases: the strongly anticoagulant phospholipase A_2 from *Naja nigricollis* venom binds to coagulation factor Xa to inhibit the prothrombinase complex. Arch Biochem Biophys;369:107–113.
7. Kini R.M. (2005) Structure-function relationships and mechanism of anticoagulant phospholipase A_2 enzymes from snake venoms. Toxicon;45:1147–1161.
8. Thunnissen M.G.M., Ab E., Kalk K.H., Drenth J., Dijkstra B.W., Kuipers O.P., Dijkman R., de Haas G.H., Verheij H.M. (1990) X-ray structure of phospholipase A_2 complexed with a substrate-derived inhibitor. Nature;347:689–691.
9. Scott D.L., White S.P., Browning J.L., Rosa J.J., Gelb M.H., Sigler P.B. (1991) Structures of free and inhibited human secretory phospholipase A_2 from inflammatory exudate. Science;254:1007–1010.
10. Chandra V., Kaur P., Jasti J., Betzel C., Singh T.P. (2001) Regulation of catalytic function by molecular association: structure of phospholipase A_2 from *Daboia russelli* pulchella ($DPLA_2$) at 1.9 Å resolution. Acta Crystallogr D Biol Crystallogr;D57:1793–1798.
11. Singh G., Gourinath S., Sharma S., Paramasivam M., Srinivasan A., Singh T.P. (2001) Sequence and crystal structure determination of a basic phospholipase A_2 from common krait (*Bungarus caeruleus*) at 2.4 Å resolution: identification and characterization of its pharmacological sites. J Mol Biol;307:1049–1059.
12. Banumathi S., Rajashankar K.R., Notzel C., Aleksiev B., Singh T.P., Genov N., Betzel C. (2001) Structure of the neurotoxic complex vipoxin at 1.4 Å resolution. Acta Crystallogr D Biol Crystallogr;D57:1552–1559.
13. Gu L., Zhang H., Song S., Zhou Y., Lin Z. (2002) Structure of an acidic phospholipase A_2 from the venom of *Deinagkistrodon acutus*. Acta Crystallogr D Biol Crystallogr;D58:104–110.
14. Matoba Y., Katsube Y., Sugiyama M. (2002) The crystal structure of prokaryotic phospholipase A_2. J Biol Chem;277:20059–20069.
15. Xu S., Gu L., Jiang T., Zhou Y., Lin Z. (2003) Structures of cadmium-binding acidic phospholipase A_2 from the venom of Agkistrodon halys Pallas at 1.9 Å resolution. Biochem Biophys Res Commun;300:271–277.
16. Xu S., Gu L., Wang Q., Shu Y., Song S., Lin Z. (2003) Structure of a King cobra phospholipase A_2 determined from a hemihedrally twinned crystal. Acta Crystallogr D Biol Crystallogr;D59:1574–1581.

17. Jasti J., Paramasivam M., Srinivasan A., Singh T.P. (2004) Structure of an acidic phospholipase A_2 from Indian saw-scaled viper (*Echis carinatus*) at 2.6 Å resolution reveals a novel intermolecular interaction. Acta Crystallogr D Biol Crystallogr;D60:66–72.
18. Lok S.M., Gao R., Rouault M., Lambeau G., Gopalakrishnakone P., Swaminathan K. (2005) Structure and function comparison of *Micropechis ikaheka* snake venom phospholipase A_2 isoenzymes. FEBS J;272:1211–1220.
19. Chandra V., Jasti J., Kaur P., Betzel C., Singh T.P. (2002) Structural basis of phospholipase A_2 inhibition for the synthesis of prostaglandins by the plant alkaloid aristolochic acid from a 1.7 Å crystal structure. Biochemistry;41:10914–10919.
20. Chandra V., Jasti J., Kaur P., Srinivasan A., Betzel C., Singh T.P. (2002) First structural evidence of a specific inhibition of phospholipase A_2 by alpha-tocopherol (vitamin E) and its implications in inflammation: crystal structure of the complex formed between phospholipase A_2 and alpha-tocopherol at 1.8 Å resolution. J Mol Biol;320:215–222.
21. Singh N., Jabeen T., Pal A., Sharma S., Perbandt M., Betzel C., Singh T.P. (2006) Crystal structures of the complexes of a group IIA phospholipase A_2 with two natural anti-inflammatory agents, anisic acid, and atropine reveal a similar mode of binding. Proteins;64:89–100.
22. Schevitz R.W., Bach N.J., Carlson D.G., Chirgadze N.Y., Clawson D.K., Dillard R.D., Draheim S.E., Hartley L.W., Jones N.D., Mihelich E.D., Olkowski J.L., Snyder D.W., Sommers C., Wery J.P. (1995) Structure-based design of the first potent and selective inhibitor of human non-pancreatic secretory phospholipase A_2. Nat Struct Biol;2:458–465.
23. Chandra V., Jasti J., Kaur P., Dey S., Perbandt M., Srinivasan A., Betzel C., Singh T.P. (2002) Design of specific peptide inhibitors of phospholipase A_2: structure of a complex formed between Russell's viper phospholipase A_2 and a designed peptide Leu-Ala-Ile-Tyr-Ser (LAIYS). Acta Crystallogr D Biol Crystallogr;D58:1813–1819.
24. Chandra V., Jasti J., Kaur P., Dey S., Perbandt M., Srinivasan A., Betzel C., Singh T.P. (2002c) Crystal structure of a complex formed between a snake venom phospholipase A_2 and a potent peptide inhibitor Phe-Leu-Ser-Tyr-Lys at 1.8 Å resolution. J Biol Chem;277:41079–41085.
25. Singh R.K., Vikram P., Makker J., Jabeen T., Sharma S., Dey S., Kaur P., Srinivasan A., Singh T.P. (2003) Design of specific peptide inhibitors for group I phospholipase A_2: structure of a complex formed between phospholipase A_2 from *Naja naja sagittifera* (Group I) and a designed peptide inhibitor Val-Ala-Phe-Arg-Ser (VAFRS) at 1.9 Å resolution reveals unique features. Biochemistry;42:11701–11706.
26. Scott D.L., Otwinowski Z., Gelb M.H., Sigler P.B. (1990) Crystal structure of bee-venom phospholipase A_2 in a complex with a transition-state analogue. Science;250:1563–1566.
27. Singh N., Jabeen T., Sharma S., Somvanshi R.K., Dey S., Singh T.P. (2004) Phospholipase A_2 as a target protein for non-steroidal anti-inflammatory drugs (NSAIDs): crystal structure of the complex formed between phospholipase A_2 and oxyphenbutazone at 1.6 Å resolution. Biochemistry;43:14577–14583.
28. Singh R.K., Ethayathulla A.S., Jabeen T., Sharma S., Kaur P., Singh T.P. (2005) Aspirin induces its anti-inflammatory effects through its specific binding to phospholipase A_2: crystal structure of the complex formed between phospholipase A_2 and aspirin at 1.9 Å resolution. J Drug Target;2:113–119.
29. Singh N., Jabeen T., Sharma S., Somvanshi R.K., Dey S., Srinivasan A., Singh T.P. (2006) Specific binding of non-steroidal anti-inflammatory drugs (NSAIDs) to phospholipase A_2: structure of the complex formed between phospholipase A_2 and diclofenac at 2.7 Å resolution. Acta Crystallogr D Biol Crystallogr;D62:410–416.
30. Jabeen T., Singh N., Singh R.K., Sharma S., Somvanshi R.K., Dey S., Singh T.P. (2005) Non-steroidal anti-inflammatory drugs as potent inhibitors of phospholipase A_2: structure of the complex of phospholipase A_2 with niflumi acid at 2.5 Å resolution. Acta Crystallogr D Biol Crystallogr;D61:1579–1586.
31. Gierse J.K., Koboldt C.M., Walker M.C., Seibert K., Isakson P.C. (1999) Kinetic basis for selective inhibition of cyclo-oxygenases. Biochem J;339:607–614.
32. Vane J.R., Botting R.M. (1998) Mechanism of action of nonsteroidal anti-inflammatory drugs. Am J Med;104:2S–8S. discussion 21S–22S.
33. Vane J.R., Bakhle Y.S., Botting R.M. (1998) Cyclooxygenases 1 and 2. Annu Rev Pharmacol Toxicol;38:97–120.
34. Boffa G.A., Boffa M.C., Winchenne J.J. (1976) A phospholipase A_2 with anticoagulant activity. I. Isolation from *Vipera berus* venom and properties. Biochim Biophys Acta;429:828–838.
35. Boffa M.C., Rothen C., Verheij H.M., Verger R., DeHaas G.H. (1980) Correlation of enzymatic activity and anticoagulant properties of phospholipase A2. In: Eaker D., Walstrom T., editors. Natural Toxins. Oxford: Pergamon Press; p. 131–138.
36. Verheij H.M., Boffa M.C., Rothen C., Bryckaert M.C., Verger R., de Haas G.H. (1980) Correlation of enzymatic activity and anticoagulant properties of phospholipase A_2. Eur J Biochem;112:25–32.
37. Callan O.H., So O.Y., Swinney D.C. (1996) The kinetic factors that determine the affinity and selectivity for slow binding inhibition of human prostaglandin H synthase 1 and 2 by indomethacin and flurbiprofen. J Biol Chem;271:3548–3554.
38. Kaplan L., Weiss J., Elsbach P. (1978) Low concentrations of indomethacin inhibit phospholipase A_2 of rabbit polymorphonuclear leukocytes. Proc Natl Acad Sci USA;75:2955–2958.
39. Lobo I.B., Hoult J.R. (1994) Groups I, II and III extracellular phospholipases A2: selective inhibition of group II enzymes by indomethacin but not other NSAIDs. Agents Actions;41:111–113.
40. Nygard G., Hudson M., Mazure G., Anthony A., Dhillon A.P., Pounder R.E., Wakefield A.J. (1995) Procoagulant and prothrombotic responses of human endothelium to indomethacin and endotoxin *in vitro*. Relevance to non-steroidal anti-inflammatory drug enteropathy. Scand J Gastroenterol;30:25–32.
41. Lyne P.D. (2002) Structure-based virtual screening: an overview. Drug Discov Today;7:1047–1055.
42. Sing N., Kumar R.P., Kumar S., Sharma S., Mir R., Kaur P., Srinivasan A., Singh T.P. (2009) Simultaneous inhibition of anti-coagulation and inflammation: crystal structure of phospholipase A_2 complexed with indomethacin at 1.4 Å resolution reveals the presence of the new common ligand-binding site. J Mol Recognit;22:437–445.
43. Wolber G., Langer T. (2005) LigandScout: 3-D pharmacophores derived from protein-bound ligands and their use as virtual screening filters. J Chem Inf Model;45:160–169.

44. Jones G., Willett P., Glen R.C., Leach A.R., Taylor R. (1997) Development and validation of genetic a algorithm for flexible docking. J Mol Biol;267:727–748.
45. Labute P. (2008) The Generalized Born/Volume Integral (GB/VI) implicit solvent model: estimation of the free energy of hydration using London dispersion instead of atomic surface area. J Comp Chem;29:1693–1698.

Note

[a]MOE, 2009.10. Montreal: Chemical Computing Group, Inc, available at: http://www.chemcomp.com/.